Developments in Compact High-Performance Synthetic Aperture Radar Systems for Use on Small Unmanned Aircraft

Evan Zaugg and Matthew Edwards
ARTEMIS, Inc.
Spanish Fork, UT 84660
801-979-6895
evan@artemisinc.net

David Long and Craig Stringham
Electrical and Computer Engineering Dept.
Brigham Young University
Provo, UT 84602
801-422-4383
long@ee.byu.edu

Abstract— The MicroASAR and SlimSAR are small, low-cost, synthetic aperture radar (SAR) systems that represent a new advancement in high-performance SAR. ARTEMIS, Inc. and Brigham Young University have employed a unique design methodology that exploits previous developments in designing the SlimSAR to be smaller, lighter, and more flexible while consuming less power than typical SAR systems. The C-band MicroASAR uses a linear-frequency-modulated continuous-wave signal to maximize SNR with a low-power transmitter. The MicroASAR was successfully deployed by NASA on a small unmanned aircraft, the Science Instrumentation Environmental Remote Research Aircraft (SIERRA) Unmanned Aircraft System (UAS), in the Arctic to image sea ice. The SlimSAR works at multiple frequency bands including L-band, X-band, and more, with LFM-CW and pulsed versions, demonstrating the utility of a small multi-band SAR.

Table of Contents

1 Introduction 1
2 Previous SAR Work 1
3 SAR System Design Methodology 2
4 Design of the MicroASAR 2
5 Deployment of the MicroASAR 5
6 Design of the SlimSAR 7
7 Conclusion 12
References 12

1. Introduction

The C-band MicroASAR and the multi-band SlimSAR are a complete, self-contained SAR systems that has been designed specifically to be small and lightweight while still being robust and capable. These characteristics make them ideal SAR systems for use on unmanned aircraft systems (UAS) and other small aircraft. These systems represent new advancements in high-performance, small, low-cost, SAR, designed by exploiting the techniques and technologies developed for previous systems, resulting in increased capability and flexibility, all in a small package.

With unmanned aircraft systems (UAS) being used more and more frequently in military, civilian, and scientific applications, providing remote-sensing, surveillance,reconnaissance, and environmental monitoring capabilities, the suite of suitable sensors available is expanding. Imaging sensors typically used on small UAS are electro-optic/infrared (EO/IR) instruments, which are limited by obstruction due to clouds, fog, dust, and smoke. On larger platforms these limitations are overcome using synthetic aperture radar (SAR) which provides high-resolution imagery day and night in all weather conditions. In addition, SAR imagery at different frequencies can provide a variety of information about an area. There are many benefits of operating multi-frequency SAR systems on small UAS, but the large size and weight of previous SAR systems preclude their use.

This paper describes the unique design of the MicroASAR and the SlimSAR, with the corresponding performance trade-offs. Examples of imagery from the MicroASAR and the SlimSAR are shown, highlighting the deployment of the MicroASAR on the NASA SIERRA UAS as part of the Characterization of Arctic Sea Ice Experiment 2009 (CASIE-09). In Section 2 we present the previous work and systems relevant to the MicroASAR and SlimSAR's heritage. In Section 3 we discuss the system design methodology. Section 4 details the design of the MicroASAR, with Section 5 describing the CASIE deployment and data processing. The SlimSAR system design is discussed in Section 6 explaining the performance trade-offs and system flexibility and showing imagery examples.

This paper summarizes the design of the MicroASAR (Section 4), its integration onto the NASA SIERRA UAS (Section 5), and its role in the CASIE mission (Section 5).

2. Previous SAR Work

The utility of having synthetic aperture radar systems that are small enough and light enough to fit on a small unmanned aircraft is apparent, however, for years such systems were beyond the reach of the available technology. The high-

[1] 978-1-4244-7351-9/11/$26.00 ©2011 IEEE.
[2] IEEEAC Paper #1292, Version 1.1, Updated 10/01/2011.

performance systems presented in this paper are build upon the advancements made during decades of work developing small SAR systems. A collaborative team of researchers from Brigham Young University (BYU) and ARTEMIS, Inc. have made a number of these advancements.

In pushing the state of the art in small, lightweight, low-power synthetic aperture radar systems BYU has developed the following airborne SAR systems:

- YSAR (1994-1996)
- YINSAR (1995-2003)
- μSAR(2004-2008)
- NuSAR (2007+)
- MicroASAR (2008+)

ARTEMIS has been supporting SAR programs for over decade with development and manufacturing. Our receivers, exciters, and up-converters are a part of Global Hawk, U-2, and ASTOR. Recent experimental programs include the UAVSAR and GLISTEN with Jet Propulsion Laboratory, the NuSAR with the Naval Research Laboratory (NRL) and Space Dynamics Laboratory (SDL), and in association with Brigham Young University (BYU), the MicroASAR. The SlimSAR is the most recent development, exploiting the technologies developed for the NuSAR and the MicroASAR.

The YSAR and YINSAR

The YSAR [1] was designed with mostly commercial off-the-shelf parts to keep costs low. The system weight was only 360 lbs, including a large battery power supply. With a center frequency of 2.1 GHz and a 200 MHz bandwidth, the system was intended for low-altitude mapping of archaeological sites. A number of areas in Israel were mapped in 1996 showing buried ruins of walls, roads, and building foundations from ancient settlements.

The development of the YINSAR [2] also used low-cost components to keep the cost and weight low. The RF subsystem was built by the engineers that would later found ARTEMIS, Inc., setting the stage for later collaborative efforts. The YINSAR had a center frequency of 9.9 GHz a 200 MHz bandwidth, and two receive channels for single-pass interferometric operation. A large portion of the system cost was the inclusion of a precision integrated GPS/IMU motion measurement system, which enabled motion compensation of the SAR imagery.

The BYU μSAR

The BYU μSAR [3] was designed and built by students. The system size was reduced to a stack of microstrip circuit boards 3”x3.4”x4” and weighing less than 4 lbs, including antennas and cabling. The system had a center frequency of 5.56 GHz, and a bandwidth up to 160 MHz. The miniaturization is made possible by using a linear-frequency modulated continuous wave signal, which allows for a high SNR while transmitting at a much lower power. The μSAR consumes 18 W and transmits 1 W. It was designed to fly at an altitude of 1000 ft or less on an unmanned air vehicle (UAV) with a 6-foot wingspan.

NuSAR

The NRL UAS SAR System (NuSAR) [4] was developed as part of NRL’s DUSTER program in a team effort with BYU, ARTEMIS, SDL, and NRL. The NuSAR is designed for UAS flight, operating at L-Band with a variable bandwidth of 500 MHz maximum (resulting in a resolution as fine as 30 cm). It is a low-power pulsed system with a peak transmit power of 25 W and is designed to operate at 2500-6000 ft above ground level (AGL). The addition of a block up/down converter extends operation to other frequency bands, with the system nominally outfitted with an X-band block converter.

3. SAR System Design Methodology

The MicroASAR is a ruggedized design based on the μSAR while the SlimSAR is based on the MicroASAR and NuSAR. The MicroASAR [5] and the SlimSAR [6] were designed using an innovative methodology [7], [8], with the goal being to find the quickest path from system requirements specification to deployment of a successful solution leaning heavily on previously developed and tested SAR systems. The existing designs were exploited to keep much of the design heritage while best meeting the system requirements. The risks associated with new, untested technologies are thus minimized.

Basing the design on an previous SAR system provided benefits for the integration and system testing process. The NuSAR and the MicroASAR were operating during the SlimSAR development period on a small, manned aircraft used as a UAS surrogate. Using the MicroASAR data from these flights, the data collection, handling, and processing methods were refined then used with very little modification for the SlimSAR. The system was therefore ready for initial flight testing as soon as the hardware was completed. Immediate flight testing on the test bed aircraft revealed necessary changes in the SAR system, the processing algorithms, and other supporting systems to ensure high quality imagery.

For the SlimSAR, the preliminary design work was completed during October 2008 with the first test flight of an LFM-CW version conducted the week of June 15, 2009. Over the next couple of weeks the system was refined in a very quick loop, with feedback from test flights prompting changes in hardware and software with immediate flight testing to verify the improved operation and provide feedback for further improvement. The pulsed version of the SlimSAR was first tested in January 2010.

4. Design of the MicroASAR

The MicroASAR uses a linear frequency-modulated (LFM) chirp generated by a direct digital synthesizer (DDS) chip. Although the μSAR used a frequency modulation scheme that ramps up then down, with each up-down cycle comprising

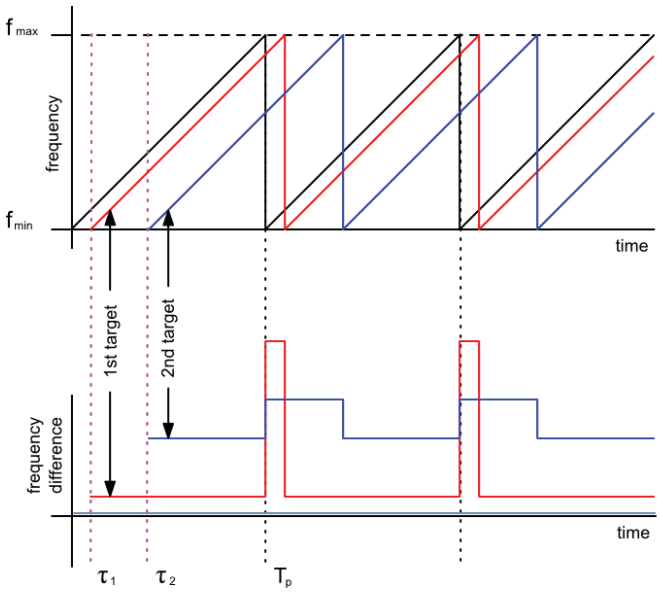

Figure 1. A line diagram showing the idealized (exaggerated) spectrogram of the received signal before (top) and after (bottom) de-chirping. Note that a delay in time translates directly to a difference in frequency.

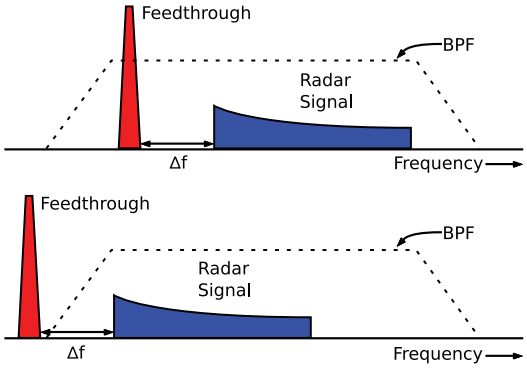

Figure 2. Representation of MicroASAR dechirped signal spectrum. A BPF is used to filter the feedthrough component by shifting the spectrum down. Δf is the frequency representation of the distance between the platform and the ground.

one pulse repetition, the MicroASAR's chirp ramps in a single direction only in order to more easily achieve high pulse repetition frequencies (PRFs). The DDS needs a few clock cycles to reset between chirps, which means that while the MicroASAR is effectively an LFM-CW radar, its transmit waveform is not strictly continuous wave (CW). Nevertheless, the benefits of LFM-CW are realized in this configuration.

LFM-CW SAR Signal

By maximizing the pulse length, an LFM-CW system is able to maintain a high SNR while transmitting with a lower peak power than a comparable pulsed SAR. Also, final processing is simplified by performing an analog "dechirping" of the signal in which the received signal is mixed with a copy of the transmitted signal. Since the waveform is an LFM chirp, the difference between the transmitted chirp and a delayed copy of itself is a frequency linearly proportional to the time of the delay. Thus, the frequencies correspond directly to the slant-range of the target and the dechirped signal is a frequency domain representation of the range-compressed SAR image. This is illustrated in Fig. 1. In the dechirped signal, near range targets have a lower frequency than far range targets. The bandwidth of this signal is much less than the transmit signal bandwidth, thus the digital sampling requirements are relaxed.

LFM-CW operation enables transmitting with less power and sampling the data at a slower rate, which can be done with hardware that is smaller, lighter, and consumes less power than traditional pulsed systems. The disadvantages are that the transmit and receive channels require separate antennas and feed-through between the antennas must be controlled. The CW scheme also has the side effect of limiting the unambiguous range that can be imaged by the sensor, and thus the altitude at which the aircraft can fly. The MicroASAR is designed for small, low-flying aircraft, so this restriction is only a small concern. The system is very flexible, however, and can be configured to transmit pulsed radar signals if needed.

Since a CW SAR system is constantly transmitting, a bistatic configuration with a separate antenna for the receive channel is used to maximize transmit-receive isolation. An undesirable side effect of bistatic, LFM-CW SAR is feedthrough between the transmit and receive antennas. This relatively strong feedthrough component dominates the low end of the dechirped spectrum and must be removed before final processing. It is desirable to remove the feedthrough component as early as possible in order to minimize the required dynamic range at the receiver and analog-to-digital converter (ADC), which would otherwise need to handle both the strong feedthrough and the weak radar returns. Feedthrough removal can be accomplished at baseband by utilizing a high-pass filter with a very low cutoff frequency, but this type of filter generally has a very long impulse response, which leads to degradation of the filtered signal. The MicroASAR removes the feedthrough component after dechirping with a surface acoustic wave band-pass filter (SAW BPF) centered at 500 MHz. The SAW BPF was selected for this purpose because of its high performance and ready availability. In order to accomplish the feedthrough removal, the frequency of the crystal oscillator, from which all signals are generated, is chosen so that the feedthrough component in the dechirped signal is mixed down to the first null of the BPF. This feedthrough removal scheme is illustrated in Fig. 2.

As seen in Fig. 2, Δf is the frequency difference between the feedthrough component and the return from nadir. We define $k_r = Bf_p$ where B is the bandwidth of the LFM chirp and f_p is the PRF. We also define Δt, the time required for a transmitted chirp to travel from the transmitting antenna to a target and back, as $\Delta t = \frac{2R}{c_0}$ where R is the slant range from

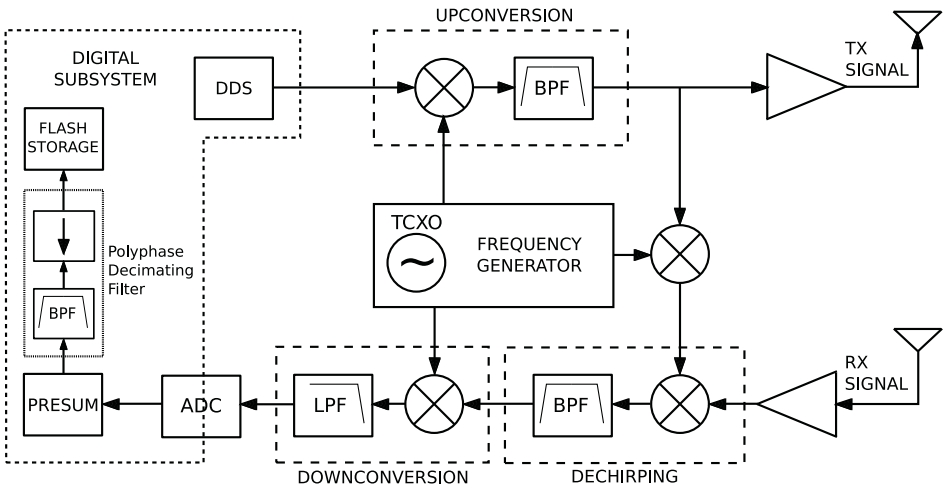

Figure 3. Simplified block diagram for the MicroASAR system. All clocks and signals are derived from the temperature compensated crystal oscillator (TCXO).

the antenna to the target and c_0 is the speed of light. Then $\Delta f = k_r \Delta t$. We label the Δt's corresponding to feedthrough and nadir Δt_{ft} and Δt_n, respectively. Then,

$$\Delta f_{min} = k_r(\Delta t_n - \Delta t_{ft}) \tag{1}$$

is the minimum Δf that places the feedthrough component in the null of the BPF while allowing the radar signal to pass through the BPF. Substituting k_r and Δt as defined above yields

$$\Delta f_{min} = \frac{2B f_{p,min}}{c_0}(R_n - \beta) \tag{2}$$

where R_n is the distance from the antenna to nadir and β is the length of the effective free-space path that the feedthrough signal takes. β is on the order of a few meters or less. Choosing Δf_{min} based on the roll-off of the BPF, the minimum PRF is

$$f_{p,min} = \frac{\Delta f_{min} c_o}{2B(R_n - \beta)} \tag{3}$$

The frequency difference between the 10 dB point and the first null of the BPF is 1.1 MHz. This is Δf in Eq. (3). We also use the values $B = 120$ MHz, $R_n = 100$ m, and $\beta = 2$ m. This yields a PRF of $f_{p,min} = 14.03$ kHz. As the altitude is increased, the difference between the feedthrough and the first radar return naturally increases so that the required PRF decreases. At $R_n = 1000$ m, for instance, the required PRF is $f_{p,min} = 1.4$ kHz. In normal SAR systems, the PRF must simply be high enough to avoid aliasing of the Doppler spectrum in slow time. The bandwidth of the Doppler spectrum is $B_D = 2v\theta_a/\lambda$ where θ_a is the azimuth beamwidth of the antenna. At reasonable velocities, this value is on the order of a few hundred Hertz so that the minimum PRF as constrained by Δf_{min} is much higher than required by Nyquist.

While these high PRFs allow us to remove the feedthrough from the dechirped signal with a BPF, they also stretch out the spectrum of the radar returns, as differences in range now translate into much greater differences in frequency. The MicroASAR limits its range to echoes that are received within one tenth of the pulse repetition interval, which limits the bandwidth of the baseband dechirped signal to 12 MHz. According to the Nyquist constraint, it would be necessary to sample this data at 24 MHz in order to avoid aliasing. Assuming 16-bit samples, this would require storing raw data at a rate of 48 MBytes/sec.

We avoid large storage rate requirements by presumming the data before storing it. As an example let's assume the system is operating at an altitude of 180 m and a velocity of 70 m/s, the minimum PRF as constrained by Δf_{min} is calculated to be $f_{p,min} = 7.8$ kHz. The Doppler bandwidth, as defined above, is $B_D = 389.1$ Hz which means that the minimum PRF to avoid Doppler aliasing is $2(389.1) = 778.2$ Hz. Presumming every 10 lines in the azimuth direction reduces the operating PRF of 7.8 kHz to an effective PRF of $f_{p,\mathit{eff}} = 780$ Hz, which still meets the constraints of the Doppler spectrum. Presumming reduces the amount of data that needs to be stored by a factor of 10. We now store the data at 4.8 MBytes/sec and still have sufficient information to reconstruct a high-quality image. As the PRF is lowered, the allowable presum factor must also be lowered, thus increasing the data rate. For this reason, the maximum data rate sets a lower bound on the PRF. In this example, the maximum storage rate of 5 MBytes/sec means that the PRF must be approximately 7.8 kHz or higher.

Using the method outlined above, the capabilities of the MicroASAR have been calculated over a range of different operating conditions. Calculated swath width versus altitude for a range of velocities is displayed in Fig. 4. These results are summarized in Table 1 along with system specifications.

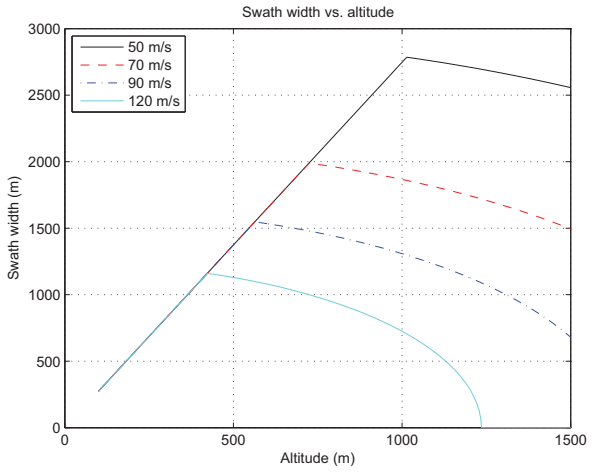

Figure 4. Maximum swath width versus altitude for different velocities. The linear first portion of the plot is limited by an antenna 3 dB beamwidth of 50°, the second portion is limited by a maximum storage rate of 5 MBytes/sec. The swath width may be increased by increasing the storage rate.

MicroASAR Hardware

The MicroASAR is completely contained in one aluminum enclosure measuring 22.1x18.5x4.6 cm. The enclosure is designed to minimize spurious emissions, self-interference, and interference from outside sources. Despite its solid metal enclosure, the entire system, including two antennas, weighs less than 3.3 kilograms. Its lightweight design makes it suitable for aircraft with payload restrictions, such as UAVs.

A simplified block diagram showing the functions of the major signal paths is given in Fig. 3. To maintain phase coherence, all signals and clocks are derived from a single temperature compensated crystal oscillator (TCXO) which has been tuned specifically so that the feedthrough component can be removed as discussed in Section 4. The DDS generates the LFM chirp, which is then upconverted, amplified, and transmitted. A copy of this transmitted chirp is frequency-shifted and mixed with the received signal to produce the dechirped signal. The dechirped signal is then downconverted to an offset video frequency and sampled. The MicroASAR actually has two receive channels to support interferometric operation.

The digital subsystem for the MicroASAR contains the DDS chip which is used to generate the LFM chirp, a high-speed 500 Msps ADC, and a Virtex 4 FPGA. The FPGA is used to control the other chips, as well as to perform simple, pre-storage processing such as presumming and filtering. Because the dechirped radar data is sampled at an offset video frequency, it is necessary to filter and downsample in order to obtain baseband data for storage. A digital bandpass filter performs the dual task of reducing quantization noise and limiting the bandwidth of the dechirped signal so that it will not alias destructively. This filter/decimate operation is accomplished by way of a polyphase decimating filter. The decimation is designed so that an aliased copy of the signal ends up at baseband, eliminating the need for a separate mixing operation. After the data has been presummed, filtered, decimated, and low-pass filtered, the baseband signal is either written to two flash memory cards, which are accessible through the front panel of the system, or streamed over Ethernet.

Table 1. **MicroASAR System Specifications**

Physical Specifications	
Transmit Power	30 dBm
Supply Power	< 35 W
Supply Voltage	+15 to +26 VDC
Dimensions	22.1x18.5x4.6 cm
Weight	2.5 kg
Radar Parameters	
Modulation Type	LFM-CW
Operating Frequency Band	C-band
Transmit Center Frequency	5428.76 MHz
Signal Bandwidth	80-200 MHz (variable)
PRF	7-14 kHz (variable)
Radar Operating Specifications	
Theoretical Resolution	0.75 m (@ 200 MHz BW)
Operating Altitude	500-3000 ft
Max. Swath Width	300-2500 m (alt. dependent)
Operating Velocity	10-150 m/s
Collection Time (for 10GB)	30-60 min (PRF dependent)
Antennas (2 required)	
Type	2 x 8 Patch Array
Gain	15.5 dB
Beamwidth	8.5°x50°
Size	35x12x0.25 cm

As previously noted, LFM-CW operation requires less power than a comparable pulsed SAR and enables hardware which is less complicated. The hardware solution provided by ARTEMIS (shown in Fig. 5), is robust enough to withstand the rigors of airborne applications while still being small and lightweight.

5. Deployment of the MicroASAR

The MicroASAR was used on the NASA Science Instrumentation Environmental Remote Research Aircraft (SIERRA) UAS [9] during a science field campaign in 2009 to study sea ice roughness and break-up in the Arctic and high northern latitudes. This mission was known as CASIE-09 (Characterization of Arctic Sea Ice Experiment 2009). CASIE combines the use of a variety of remote sensing methods, including satellite observations and UAS, to provide fundamental new insights into ice roughness on the scale of meters to tens of meters in the context of larger-scale environmental forcing. In addition, the mission offered a technological and operational testbed to demonstrate the value of autonomous vehicles for

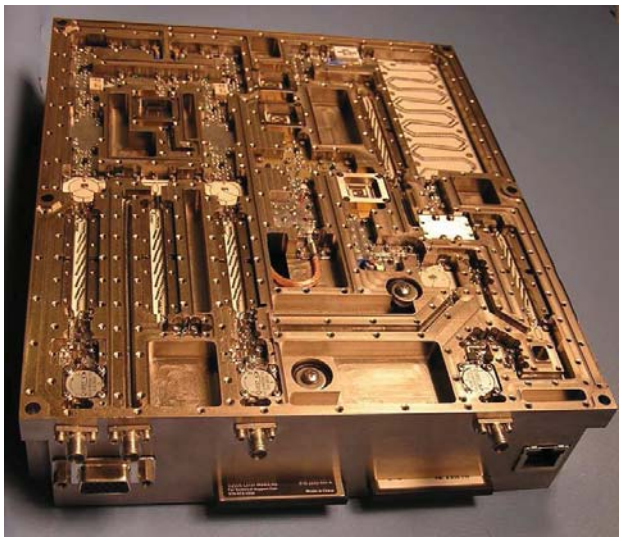

Figure 5. MicroASAR with cover removed showing RF components. Also pictured is the front panel containing RF ports, flash memory cards, serial and Ethernet connections.

long-range, long-duration remote sensing science. Five science flights covering 2923 km of sea ice were flown in July 2009.

The NASA SIERRA UAS (see Figs. 6 and 7) is an ideal platform for the MicroASAR. With a relatively large payload capacity, efficient mission planning software, and in-flight programmable autopilot, the SIERRA is perfect for a variety of data gathering missions. The SIERRA UAS is of particular value when long duration flights preclude a human pilot, or where remoteness and harshness of the environment puts pilots and manned aircraft at risk. A combination of sensors can be carried that would be too large and heavy to deploy on a single, smaller UAS. This large payload was critical in meeting the need for simultaneously acquired sea ice observations from multiple sensors. The ice pack in Fram Strait is highly dynamic, with fast ice drift and potential for ridging and rafting, so simultaneous multi-sensor observation is critical.

For the CASIE mission, the SIERRA payload consisted of

- Laser altimeter/surface height profiler (non-scanning) system consisting of two lasers acquiring simultaneous but laterally offset laser tracks, GPS, inertial measurement unit, and payload computer.
- Imaging synthetic aperture radar (the MicroASAR) with video camera.
- Three digital cameras.
- Up-looking and down-looking broadband shortwave radiation pyranometers.
- Up-looking and down-looking shortwave spectrometers.
- Down-looking temperature sensors (pyrometers).
- Temperature/Rh Sensors

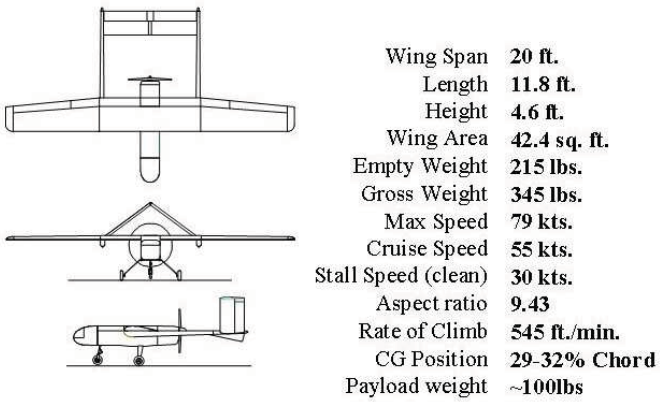

Figure 6. NASA SIERRA UAS 3-View and Specifications

The CASIE Mission

The CASIE mission was conducted as a data collection effort in support of an International-Polar-Year project titled "Sea Ice Roughness as an Indicator of Fundamental Changes in the Arctic Ice Cover: Observations, Monitoring, and Relationships to Environmental Factors", supported by NASA Cryospheric Sciences and led by Principal Investigator, Dr. James Maslanik of the University of Colorado. The project included scientists, engineers and students from the University of Colorado, Brigham Young University, Fort Hays State University and NASAs Jet Propulsion Laboratory working together with research aviation specialists from NASAs Ames Research Center. The purpose of the mission is to determine the degree to which ice-roughness monitoring via remote sensing can detect basic changes in ice conditions such as ice thickness and ice age, to investigate relationships between ice roughness and factors affecting the loss or maintenance of the perennial ice cover, and to determine how roughness varies as a function of different kinematic conditions and ice properties.

CASIE contributed to the overall project by providing an unprecedented suite of high-resolution data over a range of sea ice conditions within the Fram Strait region between northern Greenland and Svalbard. These data include surface topography observations, standard electro-optical (EO) imagery, SAR imagery, and surface reflectance and surface temperature measurements. NASA deployed the SIERRA with the MicroASAR on-board, along with a ground control station, a science team, and an operation and logistics team to collect science data in and around the Svalbard archipelago of Norway in July 2009.

Flights of the SIERRA took place from Ny-Alesund, Svalbard. This location was selected because it provides access to ice with a range of thicknesses, age, and ridging characteristics within acceptable flight range of the UAS. The SIERRA typically flew to the north and northwest, passing over open ocean and the marginal sea ice zone to target the variety of thick, old ice within the Fram Strait ice outflow region. Once

Figure 7. The NASA SIERRA UAS and the CASIE team in Ny-Alesund, Svalbard, Norway.

over the desired ice conditions, most of the flight patterns involved closely spaced, adjacent flight tracks to provide mapping coverage. The five science flights are summarized here:

- July 16 - 5hr, 49min
- July 22 - 7hr, 57min
- July 24 - 10hr, 7min
- July 27 - 8hr, 39min
- July 29 - 8hr, 15min
- 2923 km of sea ice flown

SAR Data Processing

The image formation algorithms that have been implemented for the MicroASAR and the SlimSAR include the range-Doppler (RDA), frequency-scaling (FSA), and backprojection. Primarily our processing is done using backprojection, which has often been considered the hallmark processing algorithm. Until recently it had been considered too computationally taxing to be used for general image processing. The beauty of the backprojection algorithm lies in its simplicity; backprojection can be considered the matched filter operation on the range-compressed data that uses precise knowledge of the distance from the antenna to the imaging surface to calculate the contribution of each pulse to each pixel, thus backprojection implicitly accounts for nonlinear movement and range cell migration. Furthermore because each distance and phase calculation is considered independently, backprojection easily lends itself to being computed on highly parallel processors such as the NVidia CUDA platform.

The NVidia CUDA cards provide hundreds of processing cores operating at speeds about 1.5 GHz, providing ample processing power. There is, however, very limited memory access, thus in the implementation of an algorithm it is often more important to consider the memory accesses than the computations. The backprojection algorithm starts by using a zero padded FFT to range compress and interpolate the dechirped data. Next, a thread for each pixel is created to calculate the distance from the pixel location to each antenna position in a section of the flight (to reduce global memory accesses these positions are kept in shared memory). Using these precise distances the interpolated data for each pulse is multiplied by the conjugate of its expected phase and summed together.

The speed up of this implementation varies according to the parameters of the flight, however calculations that took minutes now take seconds and the full image processing time is very comparable to frequency-domain methods. The quality of the implementation is demonstrated in the results shown in this paper.

Processing the CASIE MicroASAR Data—The MicroASAR data was stored onto Compact Flash cards and processed post flight. The SAR imagery covers a swath of sea ice about 850 meters wide with a range resolution of about 90 cm. The data was first quickly processed using the Range-Doppler Algorithm (RDA), using only rough position information that was recorded with the SAR data. Motion of the small UAS caused significant degradation to the overall SAR image quality in these first-run images. Fortunately high-precision GPS data was recorded on the CASIE platform for use with the other sensors. The data was reprocessed using high-precision backprojection after carefully aligning the GPS data, compensating for the the cable delay, and estimating the nadir height.

To make storage and processing easier the SAR data was broken into chunks where the flight path is roughly linear. The pixel locations on which to project the image were determined by estimating the height of the imaging surface to be at sea level. Then the corners of the image grid were determined using the GPS start and stop locations and the maximum range of the SAR. MicroASAR imagery, formed with the backprojection algorithm and the techniques discussed in this section, can be found in Figs. 8 and 9.

6. Design of the SlimSAR

The SlimSAR shares many of the features of the MicroASAR design, but has a number of improvements. There are LFM-CW and traditional pulsed versions of the SlimSAR, each designed for multi-frequency operation. The L-band SlimSAR core is a self-contained radar system that weighs only 6 lbs

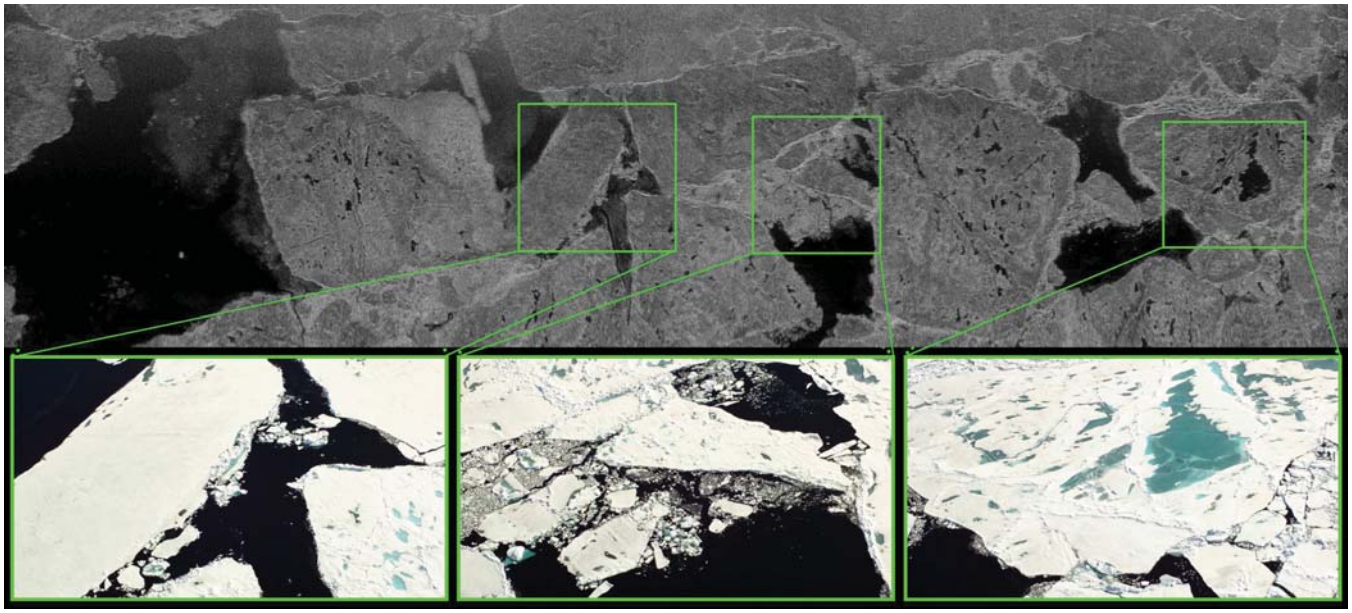

Figure 8. A series of images collected during the CASIE mission showing agreement between the MicroASAR sensor (top) and the on board video camera (bottom).

and consumes less than 150 W including a built-in motion measurement system. Additional frequency bands are made available by using a block frequency converter that weighs 2 lbs and consumes about 32 W for each additional frequency. The current test set-up has UHF and X-band capability, with additional bands in development. Add-ons to the system include a miniature data link and a gimbal for high-frequency antennas.

Delayed Mix-Down Chirp

The LFM-CW version of the SlimSAR sidesteps the range limitation imposed by the direct-dechirp of the MicroASAR (discussed in Section 4). The system does this by using two direct digital synthesizers (DDS) which generate identical SAR signals, with one delayed by the time of flight to the closest range of the desired imaging area. When the received signal is mixed with this second chirp, the bandwidth is reduced, lowering the sampling requirements, as with the direct dechirp. The difference is that with our delayed mixdown chirp we can increase the width of the imaged area while using the same sampling bandwidth.

The swath width is constrained by a number of inter-related factors:

1. The width of the intermediate frequency filter
2. The chirp rate and chirp bandwidth
3. The pulse-repetition frequency and antenna beamwidth
4. The platform altitude (AGL)
5. The maximum data rate
6. The mix-down chirp delay

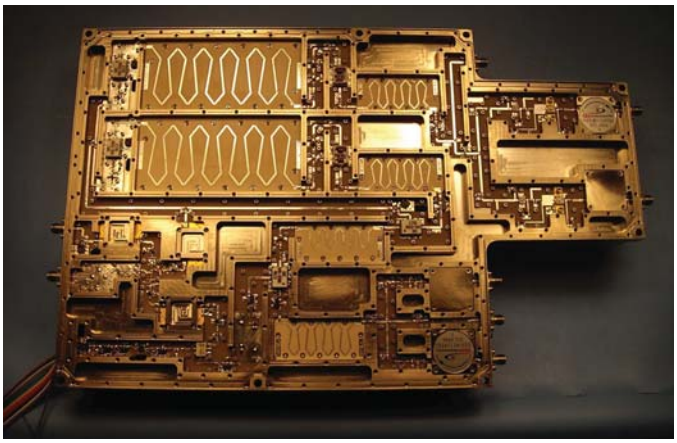

Figure 10. Photograph of SlimSAR hardware

Overall System Design Walk-Through

The core of the system is the L-band portion. An FPGA controls the variable system parameters making sure the DDS's, the ADC, and the data storage are all working together. The DDS's generate the SAR signals which are up-converted to L-band (at different frequencies). The signal is either transmitted through the L-band antenna or frequency-converted (to X-band or any other desired frequency) in one of the frequency block converters, amplified, and transmitted through the appropriate antenna.

The receive signal is amplified, and in the case of the X-band signal, down-converted to L-band. The signal is mixed with the delayed second chirp, offset in frequency, which de-chirps the signal at an intermediate frequency. A SAW band-pass filter with large out-of-band rejection removes the antenna feed-

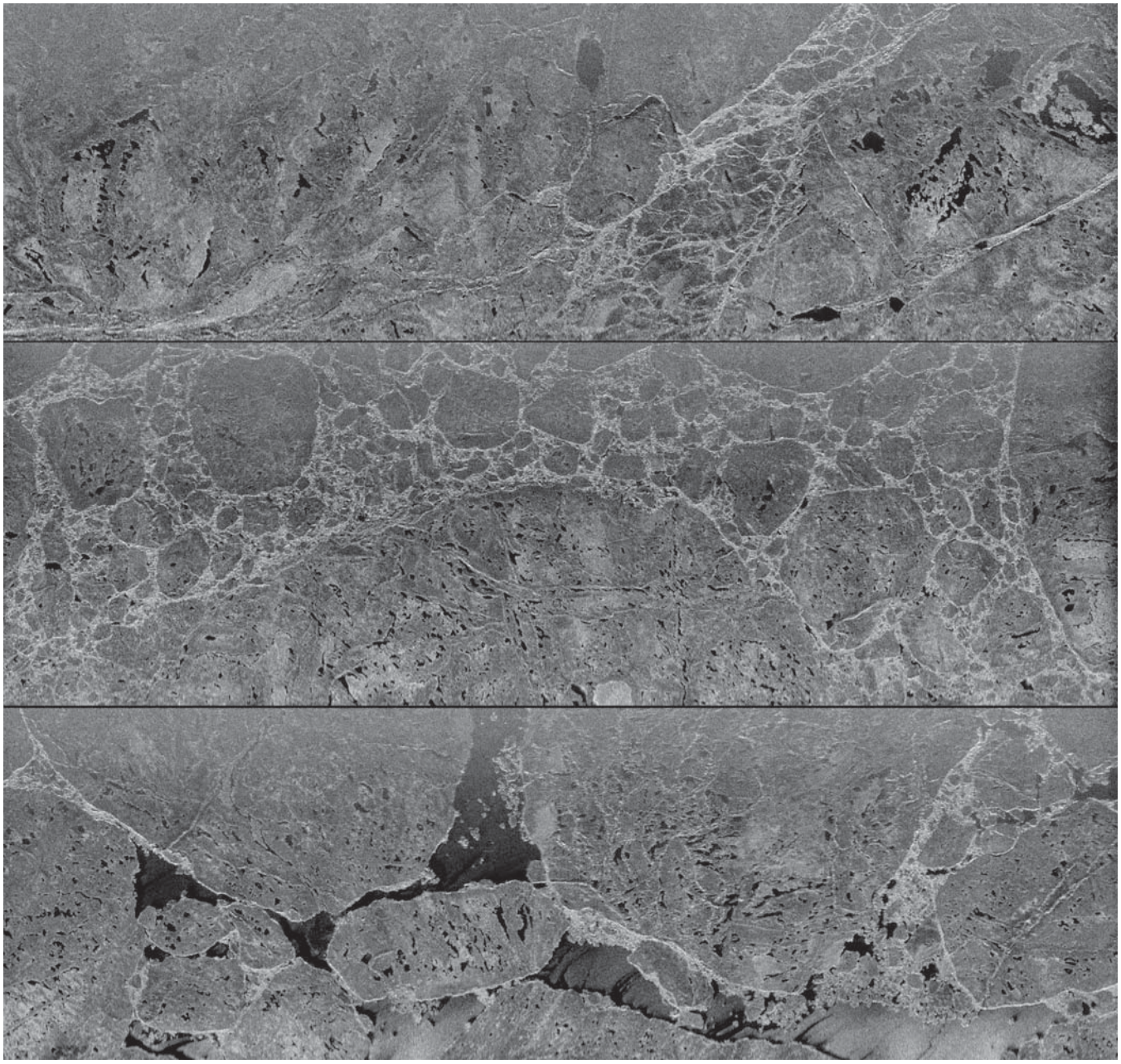

Figure 9. Examples of MicroASAR images from the CASIE mission. The three images readily show the different sea ice conditions.

through and signal returns from outside the target area. The reduced bandwidth signal is mixed-down and digitized. The digital signal is streamed via Ethernet to either on-board storage, the data-link, or an on-board processor. Range-Doppler, frequency-scaling, and backprojection algorithms have been developed for processing the data. The backprojection algorithm allows for non-linear flight paths (i.e. circular).

System specifications

The SlimSAR supports a contiguous signal bandwidth of up to 660 MHz. To accommodate restrictions in very heavily utilized spectrum bands, the bandwidth and center frequency can be adjusted and notches added. ARTEMIS operates with experimental FCC licenses at 1257.5 MHz with 85 MHz bandwidth, two X-band frequency bands, and two Ku-band frequency bands.

The built in solid-state power amplifier is designed to output 4 Watts continuous peak power for the LFM-CW model and 25 W peak for the pulsed version, sufficient for the operational altitudes of 5000-8000 feet above ground level (AGL). The system is flexible, and adding an external power amplifier can maintain higher SNR at greater altitudes. The system is also capable of transmitting and receiving horizontal and vertical

polarization for polarimetric operation.

Supporting subcomponents

There are several important subsystems which support the generation and exploitation of high-quality SAR imagery. The SlimSAR includes a built-in motion measurement system. A gimbal for small high-frequency antennas is also available. A gigabit Ethernet interface allows for the integration of a data-link for transferring the raw data to a ground station where it can be processed in near real time. The data is also stored in the 128 GB of on-board solid state storage, which is enough to record several hours of continuously collected SAR data, depending on the data rate. An on-board processor is in the works, which will provide real-time image formation for limited swath widths, and near real-time imaging for wider area coverage.

The motion measurement subsystem includes high-precision GPS and inertial measurement unit (IMU). In order to obtain high-precision inertial measurements while minimizing the necessary payload weight, 3-axis accelerometers and fiber-optic gyroscopes are integrated into the SlimSAR enclosure, eliminating the need for an extra enclosure. Additionally, at X-band (and other high-frequency bands) the antennas use a gimbaled pointing system because they have a narrow beamwidth. Data from the GPS/IMU system is fed in real time to a two-axis gimbal which controls the elevation and azimuth pointing angles of the antennas, keeping the antennas pointing perpendicular to the flight path even when the aircraft may be flying at an angle to account for wind. The gimbal allows the X-band antennas to rotate 270°, enabling the use of SlimSAR in spotlight mode and ground moving target indicator (GMTI) mode.

System Performance Trade-offs and Flexibility

Every radar system has inherent performance trade-offs, and SlimSAR is no exception. It is, however, a very flexible system; by simply adjusting some of its operational parameters, the SlimSAR can be made to operate in a wide variety of imaging situations. The pulsed version is subject to more traditional trade-offs, but the unique nature of the LFM-CW system warrants further explanation.

The width of the intermediate frequency filter—As explained in Section 4, the received signal in the SlimSAR is mixed with a copy of the transmitted signal. Through this process, time-of-flight delays are translated directly to single frequencies in the spectrum of the resulting signal. The procedure is generally referred to as de-ramping or de-chirping of the received signal because the frequency modulated chirps are converted to single tones. When a transmitted pulse scatters off a target at range R it returns to the receiver after a time-of-flight delay of $\tau = 2R/c_0$. A target at this range is represented in the dechirped signal as the single frequency

$$\Delta f = k_r \tau \tag{4}$$

where k_r is the chirp rate of the transmitted signal. The chirp rate is defined in terms of the signal bandwidth B_T and the pulse length t_p as $k_r = B_T/t_p$. In the special case of CW SAR, the pulse length is equal to the pulse repetition interval (PRI) so that the chirp rate is directly proportional to the inverse of the PRI, which is the pulse repetition frequency (PRF). The chirp rate is therefore rewritten as $k_r = B_T f_p$ where f_p is the PRF.

The SlimSAR adds an additional wrinkle to this relationship by allowing an arbitrary delay between the beginning of the transmitted signal and the beginning of the signal which is mixed with the received signal during the dechirp process. Eq. (4) is rewritten to account for this delay as

$$\Delta f = k_r (\tau - d) \tag{5}$$

The bandpass filter employed in the receiver's IF chain after the dechirp mixer selects a range of frequencies in the dechirped signal and thus effectively functions as a range-gate. Time-domain range-gating is not possible because the radar must be constantly transmitting and receiving. The range-gate function is therefore performed in the frequency domain after the dechirp process.

In order to calculate the IF filter's effect on the width of the imaged swath, we must define the width of the filter. We assume that signals which fall outside of the 3 dB bandwidth of the filter's passband are suppressed. It is also necessary to know the point in the dechirped spectrum to which signals with a zero time-of-flight delay are mapped to. A target with zero time-of-flight delay is equivalent to feeding the transmitted signal directly into the receiver. In other words, we must know the frequency in the spectrum which corresponds to $\tau = 0$ and $d = 0$. This frequency is either DC for a baseband de-chirping scheme, or it is equal to the IF used in the de-chirping process. The difference between the zero time-of-flight frequency and the upper 3 dB point of the filter's passband is defined as Δf_{max}) and the difference between the zero time-of-flight frequency and the lower 3 dB point of the filter's passband, if any, is defined as Δf_{min}.

Rewriting Eq. (5) gives an expression for maximum time-of-flight delay that is present in the filtered signal,

$$\tau_{max} = \frac{\Delta f_{max}}{k_r} + d. \tag{6}$$

Replacing Δf_{max} with Δf_{min} results in the minimum time-of-flight delay present in the filtered signal. These results are then converted to slant-range using the relation $R = c_0\tau/2$. The IF filter, therefore, directly affects the width of the imageable swath for an LFM-CW system such as the SlimSAR. The swath width is also affected by the chirp rate k_r, which is a function of the transmitted bandwidth and the PRF. The dechirp delay d does not affect the width of the swath, but rather where it physically begins and ends.

The chirp rate and chirp bandwidth—As described above, the chirp rate in an LFM-CW SAR is a function of the signal

bandwidth and the PRF. The definition is reprinted here for convenience

$$k_r = B_T f_p. \tag{7}$$

The bandwidth of the transmitted signal is generally made as wide as possible because the resolution of the final image is inversely proportional to this value. The chirp rate is modified by changing the PRF at which the radar operates. A lower PRF results in a lower chirp rate, which in turn results in a more compact dechirped spectrum as per Eq. (4).

The pulse-repetition-frequency and antenna beamwidth—A SAR system relies on the Doppler shift created while moving past a target to focus in the along-track direction. The Doppler signal is sampled in the along-track by the PRF, which must therefore be high enough to properly record the entire Doppler bandwidth. The Doppler bandwidth is dependent on the velocity of the platform, v, as well as the wavelength of the transmitted signal, λ. Because the Doppler shift increases as the azimuth angle in the along-track direction is increased, the maximum Doppler bandwidth is calculated at the edges of the antenna's azimuth beamwidth, θ_a. A good approximation for the Doppler bandwidth is

$$f_D = \frac{2v\theta_a}{\lambda}. \tag{8}$$

Eq. (8) gives a lower bound on the operational PRF of the SAR system. The chirp rate and swath width can then be calculated for this lower bound.

The platform altitude (AGL) and dechirp delay—Platform altitude in a traditional pulsed SAR system is governed mainly by the system's transmit power. The radar signal must be transmitted with enough power to obtain a signal-to-noise ratio (SNR) which is sufficient to image intended targets. For an LFM-CW system, it is also necessary to ensure that the maximum imageable slant-range, as calculated in Eq. (6), produces the desired swath width at the given altitude. A traditional LFM-CW SAR, in which the dechirp delay d is zero, experiences a fundamental limit on platform altitude because the dechirped spectrum has a finite bandwidth and the PRF (and thus the chirp rate) is limited by the Doppler sampling requirement. With the dechirp delay equal to zero, a typical LFM-CW SAR is forced to image the space between the platform and the ground along with the desired swath. If the platform operates too high, the entire sampled slant range may be composed of space between the platform and the ground.

SlimSAR overcomes this limitation by introducing the delay d between the beginning of the transmitted pulse and the beginning of the pulse used for dechirp mixdown. This arbitrary delay does not change the width of the imageable swath, but rather changes its location relative to the platform. Increasing the dechirp delay shifts the spectrum of the dechirped signal down. Since frequency in the dechirped signal translates directly to slant range, this means that targets at a higher slant range will fall within the passband of the IF filter. Thus the SlimSAR can be configured to image a swath of a certain width from almost any altitude simply by increasing the dechirp delay and transmit power.

The maximum data rate— The SlimSAR uses an analog dechirp process to partially compress the SAR data before sampling and storage. It is therefore only necessary to store samples at a rate which is high enough to reliably digitize the bandwidth of the dechirped signal instead of the bandwidth of the transmitted signal. Much in the same way that the data rate of a pulsed SAR can be reduced by employing a range-gate to narrow the imaged swath, the data rate of the SlimSAR may be reduced by decreasing the bandwidth of the dechirped signal and sampling at a lower rate. The same effect can be achieved by increasing the operation PRF, which stretches the dechirped spectrum, and then averaging adjacent received pulses in order to reduce the effective PRF.

The SlimSAR contains a relatively wide IF filter and samples at an offset video frequency so that filtering, downsampling, and presumming operations can be performed digitally. This gives the device a great deal of flexibility when making the trade-off between wide swath images and low data rate.

Example Operating Configurations—In order to illustrate the flexibility of the SlimSAR, examples of possible operating configurations are given here. The system parameters can be tailored to meet varying requirements for swath width, altitude, data rate and other constraints.

When operating at L-band with a 185 MHz bandwidth, the L-band antennas are quite small, and have an azimuth beamwidth of 50 degrees. The platform is at 5000 ft. AGL and flying at a speed of 100 knots. Eq. (8) is used to calculate the minimum PRF which prevents aliasing in the Doppler domain. The dechirped spectrum is filtered to 12 MHz. Using Eqs. (6) and (7), the maximum possible swath width is calculated to be approximately 11 km in slant range. This result assumes that all 12 MHz of the dechirped spectrum is sampled at slightly more than Nyquist, which results in slightly over 24 Msamp/sec. If samples are stored with a precision of two bytes, the resulting data rate is nearly 50 Mbytes/sec.

In order to reduce the data rate, the bandwidth of the dechirped signal may be narrowed. This results in a narrower swath, which is the obvious trade-off. A swath that is 2 km in slant range, for instance can be obtained with a data rate of close to 7 Mbytes/sec. Even lower data rates may be obtained by narrowing the Doppler bandwidth by slowing the platform, lengthening the antenna, or filtering the data after sampling. In this way, data rates significantly lower than 5 Mbytes/sec may be obtained. It is important to note that with the delayed dechirp the 2 km slant range need not extend from the aircraft toward the ground, but can be made to begin at any arbitrary point on the ground and extend for 2 km. For this reason, the SlimSAR is limited in altitude only by its transmit power and can be configured to operate at a much wider range of

Figure 11. At left, an optical photograph (courtesy of the State of Utah), of an area at the north end of Spanish Fork, Utah is shown. At right an 85 MHz bandwidth, pulsed, HH-pol, L-band SlimSAR image is shown. The scene is illuminated from the top and measures 1.45 km by 2 km.

altitudes than previous LFM-CW systems.

Unmanned aircraft are particularly useful when long duration flights preclude a human pilot, or where remoteness and harshness of the environment puts pilots and manned aircraft at risk. Autonomously controlled vehicles can often conduct missions lasting more than 20 hours. With ample on-board storage, the SlimSAR can collect SAR data throughout the duration of the mission.

Sample SAR Imagery

The SlimSAR has been flown in a variety of locations. In Fig. 11, an area at the north end of Spanish Fork, Utah is imaged with the pulsed version of the SlimSAR. In Fig. 13, sample multi-frequency imagery from the LFM-CW SlimSAR and the MicroASAR, collected near Everett, WA, is shown.

7. Conclusion

The advantages of a strong design heritage combined with rapid testing and integration are evident in the design of the MicroASAR and the SlimSAR. For the SlimSAR, the quick schedule of going from initial concept designs to flight testing within nine months has demonstrated the utility of our design methodology. The value of a UAS operated small synthetic aperture radar has been demonstrated. The compact, flexible design of the MicroASAR and the SlimSAR made them ideal for deployment on UAS based missions. Using the MicroASAR on the SIERRA has opened the way for many other applications that would be well served by utilizing a small SAR on a UAS. Current testing is aimed at proving and refining the systems. The flexible design allows for future modifications such as alternative frequencies, higher bandwidths, and specific applications such as GMTI, interferometry, littoral and maritime modes.

References

[1] D.G. Thompson, D.V. Arnold, D.G. Long, G.F. Miner, T.W. Karlinsey, A.E. Robertson, "YSAR: a compact, low-cost synthetic aperture radar," in *Proc. Int. Geoscience and Remote Sensing Symp.*, vol.1, pp.386-388, Aug 1997.

[2] D.G. Thompson, A.E. Robertson, D.V. Arnold,

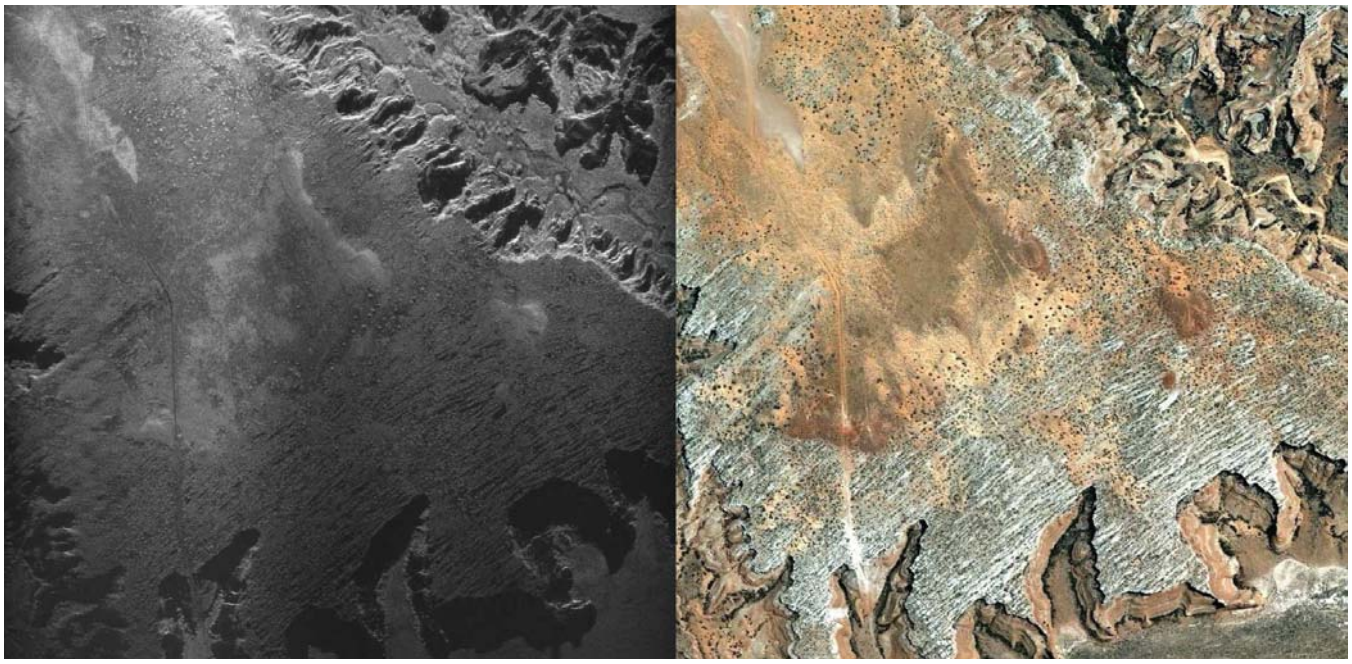

Figure 12. An area of Arches National Park shown in a X-band SlimSAR image at left and an optical photograph (courtesy of the State of Utah) at right. The X-band data has a bandwidth of 237 MHz.

D.G. Long, "YINSAR: a compact, low-cost synthetic aperture radar," in *1999 IEEE Radar Conference* pp.221-226, 1999.

[3] E.C. Zaugg, D.L. Hudson, and D.G. Long, "The BYU μSAR: A Small, Student-Built SAR for UAV Operation", in *Proc. Int. Geosci. Rem. Sen. Symp.*, Denver Colorado, pp.411-414, Aug. 2006.

[4] E.C. Zaugg, D.G. Long, and M.L. Wilson, "Improved SAR Motion Compensation without Interpolation", in *Proc. 7th European Conference on Synthetic Aperture Radar*, Friedrichshafen, Germany, v.3, pp.347-350, June, 2008.

[5] M. Edwards, D. Madsen, C. Stringham, A. Margulis, and B. Wicks, "MicroASAR: A Small, Robust LFM-CW SAR for Operation on UAVs and Small Aircraft", in *Proc. Int. Geosci. Rem. Sen. Symp.*, Boston, Mass, July, 2008.

[6] E. Zaugg, M. Edwards, A. Margulis, "The SlimSAR: A small, multi-frequency, Synthetic Aperture Radar for UAS operation," in *2010 IEEE Radar Conference* pp.277-282, May 2010.

[7] M.C. Edwards, "Design of a Continuous-Wave Synthetic Aperture Radar System with Analog Dechirp", Master's Thesis, Brigham Young University, April 2009.

[8] M.C. Edwards, E.C. Zaugg, D.G. Long, R. Christiansen, and A. Margulis, "A Small, Manned Aircraft as a Testbed for Radar Sensor Development," in *Defense, Security+Sensing, Proceedings of SPIE*, Vol. 7308, 7 pp., 12 Apr 2009.

[9] Fladeland, M. M., Berthold, R., Monforton, L., Kolyer, R., Lobitz, B., & Sumich, M., "The NASA SIERRA UAV: A new unmanned aircraft for earth science investigations", American Geophysical Union, Fall Meeting 2008, abstract B41A-0365.

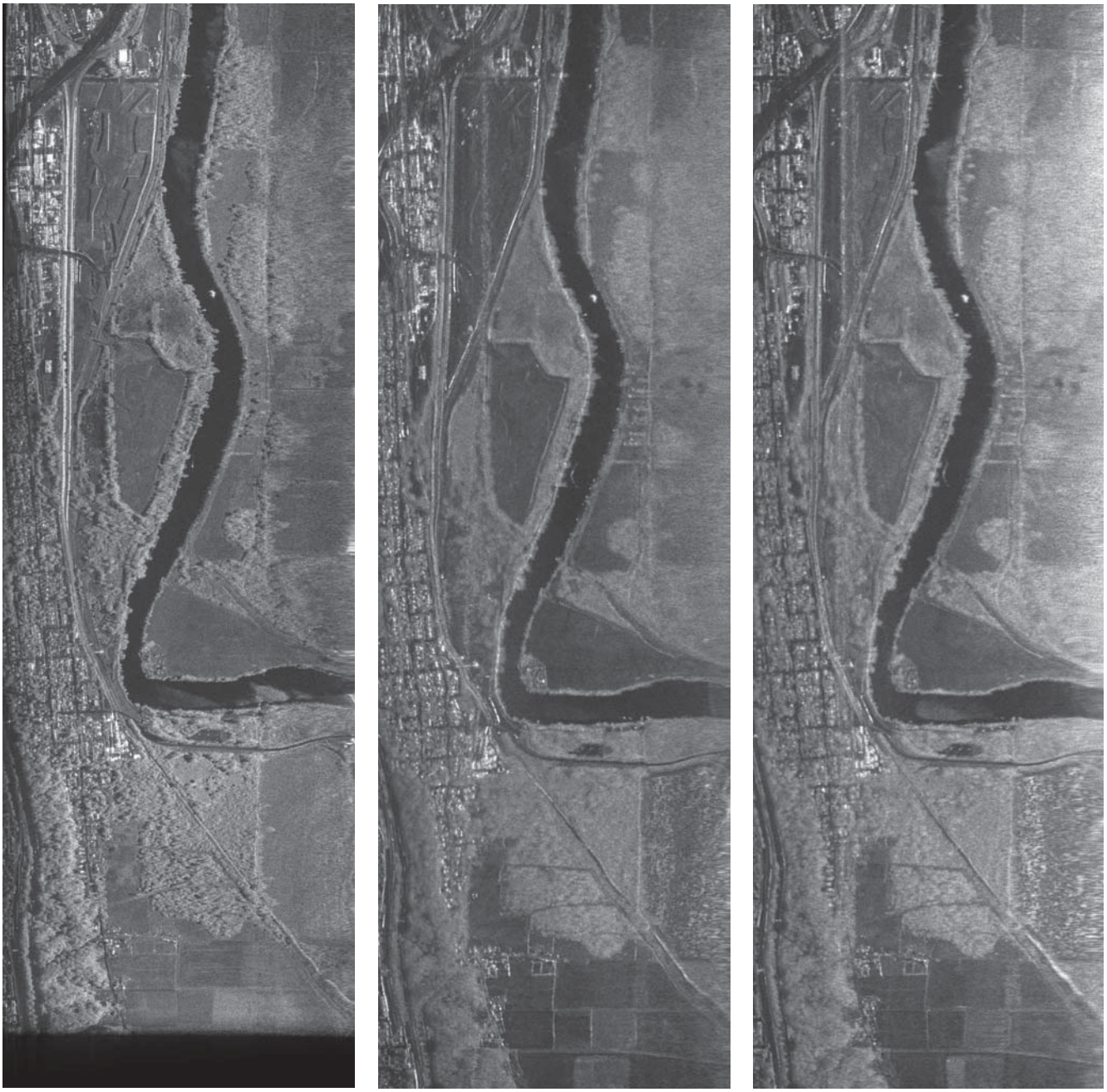

Figure 13. Simultaneously collected SAR images of an area south of Everett, Washington (the scene is illuminated from the right). The leftmost image is a C-band MicroASAR image with a range resolution of 88 cm. The center image is an L-band HH-pol SlimSAR image with the rightmost being L-band VV-pol SlimSAR image. The SlimSAR L-band images have a range resolution of 1.76 m, corresponding to the 85 MHz bandwidth. The area shown is 1.4 km wide by 4.2 km long.